Structural Characterization of CeO_2-TiO_2 and V_2O_5/CeO_2-TiO_2 Catalysts by Raman and XPS Techniques

Benjaram M. Reddy* and Ataullah Khan

Inorganic and Physical Chemistry Division, Indian Institute of Chemical Technology, Hyderabad−500 007, India

Yusuke Yamada and Tetsuhiko Kobayashi

National Institute of Advanced Industrial Science and Technology (AIST), Special Division of Green Life Technology, 1-8-31 Midorigaoka, Ikeda, Osaka 563-8577, Japan

Stéphane Loridant and Jean-Claude Volta

Institut de Recherches sur la Catalyse−CNRS, 2 Avenue A. Einstein, 69626 Villeurbanne Cedex, France

Received: February 24, 2003

Structural characteristics of ceria−titania and vanadia/ceria−titania mixed oxides have been investigated using X-ray powder diffraction (XRD), Raman spectroscopy (RS), and X-ray photoelectron spectroscopy (XPS) techniques. The (1:1 mole ratio) mixed oxide was obtained by a coprecipitation method, and a nominal 5 wt % V_2O_5 was deposited over its surface by a wet impregnation technique. Both of the materials were then subjected to thermal treatments from 773 to 1073 K and were characterized by the above-mentioned techniques. The XRD results suggest that the CeO_2-TiO_2 mixed oxide calcined at 773 K primarily consists of poorly crystalline CeO_2 and TiO_2-anatase phases and that a better crystallization of these oxides occurs with increasing calcination temperature. The "*a*" cell-parameter values suggest some incorporation of titanium into the ceria lattice. Impregnation of vanadia on ceria−titania enhances the crystallization of CeO_2 and TiO_2 oxides. However, no crystalline V_2O_5 could be observed from XRD and RS measurements. Furthermore, the dispersed molecular vanadium oxide (polyvanadate), evidenced by Raman measurements, interacts preferentially with the CeO_2 portion of the mixed oxides and forms the $CeVO_4$ compound at higher calcination temperatures. The XRD and RS results provide direct evidence about the formation of $CeVO_4$. The XPS electron-binding energies indicate that ceria, titania, and vanadia are mainly in their highest oxidation states, Ce(IV), Ti(IV), and V(V). The formation of Ce(III) has also been noticed in both CeO_2-TiO_2 and V_2O_5/CeO_2-TiO_2 samples at all temperatures.

Introduction

Ceria-based materials have been receiving enormous attention recently owing to their broad range of applications in various fields.[1] CeO_2 is a well-known additive in the so-called three-way catalysts for automobile exhaust treatment.[2] In particular, supported CeO_2 and CeO_2-based mixed oxides are the effective catalysts for the reactions of oxidation of different hydrocarbons and for the removal of total organic carbon from polluted waters from different sources.[3−6] The presence of CeO_2 promotes various catalytic reactions such as CO_2 activation,[7] CO oxidation,[3] and CO/NO removal.[8] In all of these applications, two features are mainly responsible for making CeO_2 a promising material for use either as a support or as an active catalyst. These are (a) the redox couple Ce^{3+}/Ce^{4+}, with the ability of ceria to shift between CeO_2 and Ce_2O_3 under oxidizing and reducing conditions, respectively, and (b) the ease of formation of labile oxygen vacancies and particularly the relatively high mobility of bulk oxygen species.[9] However, pure ceria is known to be poorly thermostable and undergoes rapid sintering under high-temperature applications, thereby loosing oxygen buffer capacity.[10,11] Therefore, there are several attempts in the literature to overcome this problem. One approach among them is the substitution of another metal or metal oxide into the ceria lattice, thereby facilitating the formation of mixed oxides.[12−17] Replacing cerium ions by cations of different size and/or charge modifies ion mobility inside the modified lattice, resulting in the formation of a defective fluorite-structured solid solution. Such modifications in the defect structure of ceria confer new properties to the catalyst such as better resistance to sintering at high temperatures and high catalytic activity for various reactions.[18] The mixing of two different oxides also adds another parameter because they are liable to form new stable compounds that may lead to totally different physicochemical properties and catalytic behavior.[17]

Motivated by the favorable characteristics of ceria-based mixed oxides or solid solutions, their preparation and characterization has been the objective of a great number of investigations recently. There are several studies in the literature on the dispersion and surface structure of V_2O_5 on TiO_2 and CeO_2 single oxides.[19−21] However, there is no report, to the best of our knowledge, on the nature of V-oxide species and their chemical stability on CeO_2-TiO_2 mixed oxides. Both cerium and titanium cations have multiple stable oxidation states, and the CeO_2 and TiO_2 surfaces can be relatively easily reduced.

* Corresponding author. E-mail: bmreddy@iict.ap.nic.in.

10.1021/jp0344601 CCC: $25.00
Published on Web 05/10/2003

Vanadium oxide is also a well-known redox material used in many industrial catalysts for selective oxidation and ammoxidation reactions.[22−29] Therefore, an effort has been made in the present study to understand the evolution and physicochemical characteristics of CeO_2-TiO_2 and V_2O_5/CeO_2-TiO_2 mixed oxides of great commercial significance for various purposes. The CeO_2-TiO_2 mixed oxide was prepared by a homogeneous coprecipitation method and was impregnated with a nominal 5 wt % V_2O_5. The CeO_2-TiO_2 and V_2O_5/CeO_2-TiO_2 samples were subjected to thermal treatments from 773 to 1073 K and were investigated by means of X-ray diffraction (XRD), Raman spectroscopy (RS), X-ray photoelectron spectroscopy (XPS), and other techniques.

Experimental Section

Preparation of Samples. The CeO_2-TiO_2 (1:1 mole ratio based on oxides) mixed oxide was prepared from $CeCl_3 \cdot 7H_2O$ (99.0%, Aldrich) and $TiCl_4$ (99.9%, Aldrich) by hydrolysis with aqueous ammonia solution. The cerium chloride salt was dissolved in distilled water to the desired concentration (0.1 M). To make titanium chloride solution, $TiCl_4$ was first digested in cold concentrated HCl and then diluted with distilled water. To the cerium and titanium chloride mixture solutions, dilute liquid ammonia was added dropwise with vigorous stirring until the precipitation was complete. The gel product was heated slowly to 363−368 K on a hot plate with vigorous stirring to facilitate aging. The product was filtered off and washed several times with distilled water until no chlorides could be detected with Ag^+ in the filtrate. The obtained cake was oven dried at 393 K for 12 h and finally calcined at 773 K for 5 h. Some portion of the calcined mixed oxide was once again heated at 873, 973, and 1073 K for 6 h. The V_2O_5/CeO_2-TiO_2 sample, containing 5 wt % V_2O_5 to obtain a theoretical monolayer coverage on the support surface,[24] was prepared by a standard wet impregnation method from NH_4VO_3 (99%, Fluka) dissolved in aqueous oxalic acid solution (1 M). To this aqueous solution, the finely powdered calcined (773 K) CeO_2-TiO_2 support was added. The excess water was evaporated on a water bath, and the resulting material was oven dried at 393 K for 12 h and subsequently calcined at 773 K for 5 h in an oxygen atmosphere. Some portion of the finished catalyst was once again heated at 873, 973 and 1073 K for 5 h.

Characterization Techniques. Powder X-ray diffraction (XRD) patterns were recorded on a Siemens D-500 diffractometer using a nickel-filtered Cu Kα (0.15418 nm) radiation source. The intensity data were collected over a 2θ range of 3−80° with a 0.02° step size using a counting time of 1 s per point. Crystalline phases were identified by comparison with the reference data from ICDD files. The average crystallite size of CeO_2 was estimated with the help of the Debye−Scherrer equation using the XRD data of all prominent lines.[30]

The Raman spectra were obtained on a DILORXY spectrometer equipped with a liquid-nitrogen-cooled CCD detector. The emission line at 514.5 nm from an Ar^+ laser (Spectra Physics) was focused on the sample under a microscope, and the analyzed spot was $\sim$1 μm. The power of the incident beam on the sample was 3 mW. The time of acquisition was adjusted according to the intensity of the Raman scattering. The wavenumber values reported from the spectra are accurate to within 2 cm^{-1}.

The BET surface areas were determined by N_2 adsorption using a Micromeritics Gemini 2360 instrument. Prior to analysis, the samples were oven dried at 393 K for 12 h and flushed with argon gas for 2 h.

TABLE 1: BET Surface Area and Crystallite Size Measurements of CeO_2 in CeO_2-TiO_2 and V_2O_5/CeO_2-TiO_2 Samples Calcined at Different Temperatures

sample	BET SA ($m^2\ g^{-1}$)	crystallite size (nm)	*a* cell parameter[a] (Å)
	773 K		
CeO_2-TiO_2	59	10.0	5.40
V_2O_5/CeO_2-TiO_2	44	12.9	nd[b]
	873 K		
CeO_2-TiO_2	51	10.7	5.40
V_2O_5/CeO_2-TiO_2	38	14.6	nd
	973 K		
CeO_2-TiO_2	42	11.8	5.37
V_2O_5/CeO_2-TiO_2	29	16.8	nd
	1073 K		
CeO_2-TiO_2	31	14.1	5.37
V_2O_5/CeO_2-TiO_2	14	22.3	nd

[a] Obtained per the procedure in refs 28 and 29. [b] Not determined because of composition heterogeneity.

The XPS measurements were performed on a Shimadzu (ESCA 3400) spectrometer by using Mg Kα (1253.6 eV) radiation as the excitation source. Charging of the catalyst samples was corrected by setting the binding energy of the adventitious carbon (C 1s) to 284.6 eV.[31,32] The XPS analysis was done at ambient temperature and pressures typically on the order of less than 10^{-6} Pa. Prior to analysis, the samples were outgassed in a vacuum oven overnight.

Results and Discussion

The N_2 BET surface areas of CeO_2-TiO_2 and V_2O_5/CeO_2-TiO_2 samples calcined at various temperatures are shown in Table 1. The CeO_2-TiO_2 mixed oxide calcined at 773 K exhibited a BET surface area of 59 $m^2\ g^{-1}$. As can be observed from Table 1, there is a decrease in the specific surface area with increasing calcination temperature. This is primarily due to the sintering of the samples at higher calcination temperatures. Additionally, compound formation between ceria and titania with varying stoichiometries at higher calcination temperatures cannot be ruled out. This aspect has been elaborated on in subsequent paragraphs. The 5% V_2O_5/CeO_2-TiO_2 sample calcined at 773 K exhibited a BET surface area of 44 $m^2\ g^{-1}$. With increasing calcination temperature, a substantial decrease in the surface area can be observed. The decrease in the surface area after impregnating with vanadium pentoxide and subjecting the samples to higher calcination temperatures could be due to various factors such as penetration of the dispersed vanadium oxide into the pores of the support, thereby narrowing its pore diameter and blocking some of the pores and solid-state reactions between the dispersed vanadium oxide and the supporting oxides.[24,33,34] The XRD measurements presented in the succeeding paragraphs provide evidence for the latter possibility.

Figure 1 shows the X-ray powder diffraction patterns of the CeO_2-TiO_2 sample calcined at different temperatures. The XRD measurements provide typical diffraction patterns of cubic CeO_2 (PDF-ICDD 34-0394) along with a few less-intense peaks due to the TiO_2 anatase phase (PDF-ICDD 21-1272). With increasing calcination temperature, a slight increase in the intensity of the lines due to both of these phases can be observed. Preuss and Gruehn reported various Ce−Ti−O oxides, namely, Ce_2TiO_5, $Ce_2Ti_2O_7$, and $Ce_4Ti_9O_{24}$, by heating the appropriate mixtures of solids containing Ce and Ti at 1523 K.[35] However, no such crystalline phases could be seen in the present study. The absence of crystalline Ce−Ti−O compounds may be due to a different preparation method adopted and lower calcination

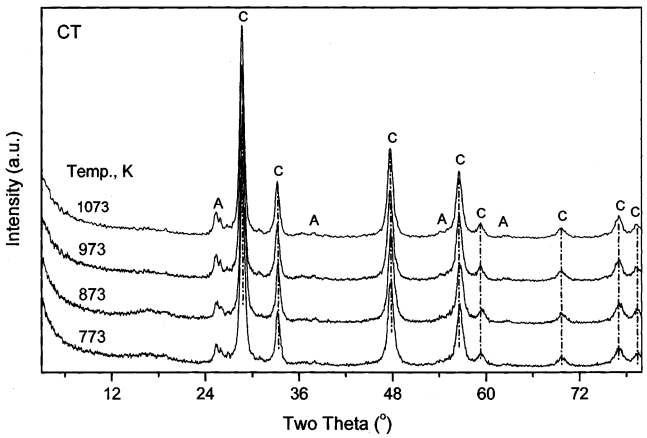

Figure 1. X-ray powder diffraction patterns of CeO_2-TiO_2 (CT) calcined at different temperatures: (C) Lines due to CeO_2; (A) lines due to TiO_2 anatase.

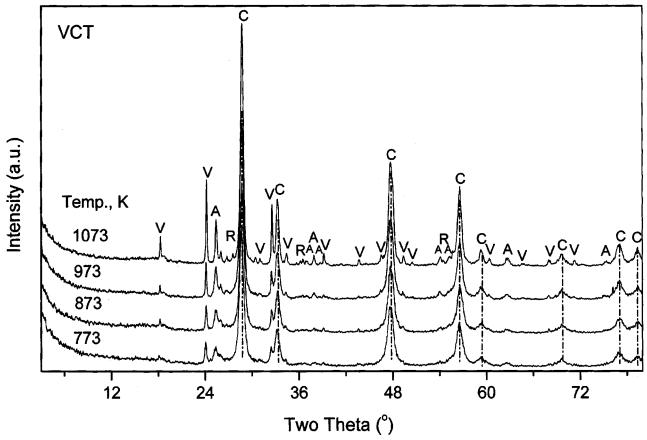

Figure 2. X-ray powder diffraction patterns of 5 wt % V_2O_5/CeO_2-TiO_2 (VCT) calcined at different temperatures: (C) Lines due to CeO_2; (A) lines due to TiO_2 anatase; (R) lines due to TiO_2 rutile; (V) lines due to $CeVO_4$.

temperatures employed in the present investigation. It is an established fact in the literature that the transformation of anatase to rutile is thermodynamically feasible beyond 873 K in impurity-free TiO_2 samples.[24,36] In the present study, there is no evidence for the formation of the rutile phase even up to 1073 K. It appears from the present results that the anatase-to-rutile phase transformation is somehow inhibited in the CeO_2-TiO_2 mixed oxides. As explained by Lin and Yu,[37] this phenomenon could be due to the stabilization of anatase by the surrounding cerium ions through the formation of Ce−O−Ti bonds. At the interface, titanium atoms are expected to substitute for cerium in the lattice of the cerium oxide to form octahedral Ti sites. The interaction between the tetrahedral Ti and octahedral Ti inhibits the phase transformation to rutile.[36] Anderson and Bard offered an analogous explanation for TiO_2-SiO_2 mixed oxides where a similar inhibition of anatase-to-rutile phase transformation was observed.[38]

The XRD patterns of a 5% V_2O_5/CeO_2-TiO_2 sample calcined at various temperatures are presented in Figure 2. Along with the prominent diffraction lines of cubic CeO_2 and the TiO_2 anatase phase, a few new diffraction peaks that can be attributed to the formation the $CeVO_4$ compound (PDF-ICDD 12-0757) are also observed. The intensity of all of these lines increased with increasing calcination temperature. No diffraction lines due to crystalline V_2O_5 are observed. A few lines with less intensity can be seen at 1073 K; these could be assigned to the TiO_2 rutile phase (PDF-ICDD 21-1276). There are also some weak extra lines that cannot be assigned to any known crystalline compounds. The absence of the crystalline V_2O_5 phase and the preferential formation of the $CeVO_4$ compound indicates that the dispersed vanadium oxide selectively interacts with the ceria portion of the CeO_2-TiO_2 mixed oxide and forms this stable oxide. It is a well-known fact in the literature that dispersed vanadium oxide on titania anatase accelerates the phase transformation from anatase to rutile. During this phase transformation, some of the V_2O_5 is reduced and gets incorporated into the rutile structure as $V_xTi_{(1-x)}O_2$ (rutile solid solution).[24] The preferential formation of the $CeVO_4$ compound at $T \geq 773$ K because of solid-state reactions between the dispersed vanadium oxide and the ceria portion of the CeO_2-TiO_2 mixed oxide seems to be an interesting observation from this study. The formation of the $CeVO_4$ phase can be explained by taking into account the charge-to-radius ratio of the mixed oxides as envisaged by Bond et al.[24] The formation of surface compounds or unidimensional layers of vanadium oxide on various oxide supports has been related to the ratio of the charge of the support cation to the sum of the radii of cation and oxide ions (q/r).[24] Normally, lower q/r ratios favor surface compound formation.[24] The q/r ratio for vanadia−ceria combination is lower because the radius of Ce^{4+} (0.97 Å) is higher than that of Ti^{4+} (0.64 Å). Therefore, the dispersed vanadium oxide is expected to interact selectively with the ceria portion of the mixed oxide, thereby leading to the formation of a crystalline $CeVO_4$ surface compound. The PZC (point of zero charge or pH at surface neutrality) values reported in the literature also support the above observation.[39,40] The PZC of ceria (8.1±0.1) is much higher than that of titania (5.9±0.1), making it more basic. Therefore, a highly feasible acid−base interaction can be expected between the dispersed vanadium oxide and ceria, leading to the formation of the $CeVO_4$ compound.

The crystallite size (D_{XRD}) of CeO_2 in various samples as a function of calcination temperature is summarized in Table 1. It appears from Table 1 that the CeO_2 crystallization depends both on the calcination temperature and the presence of dispersed vanadium oxide over its surface. An increase in the crystallite size of CeO_2 is observed with increasing calcination temperature, the increase being greater in the case of V_2O_5/CeO_2-TiO_2 samples. This is due to the accelerating effect of dispersed vanadium oxide on the crystallization of ceria, a well-known fact documented in the literature.[24,36,41,42] The *a* cell-parameter values for the CeO_2 (111) base peak, calculated using the cubic indexation method, are also presented in Table 1.[43,44] The lattice parameters were estimated to determine whether Ti^{4+} could enter into the CeO_2 lattice, resulting in the formation of solid solutions. The *a* cell-parameter values obtained at 773 and 873 K are in good agreement with the pure CeO_2 (100%) phase.[44] A subsequent decline in the *a* cell-parameter values with increasing calcination temperature can be taken as evidence for the substitution of Ti^{4+} in the ceria unit cell because the Ti^{4+} ionic radius (0.64 Å) is smaller than that of Ce^{4+} (0.97 Å).

The Raman spectra of CeO_2-TiO_2 and V_2O_5/CeO_2-TiO_2 samples calcined at different temperatures are shown in Figures 3 and 4, respectively. As presented in Figure 3, the Raman spectrum of the CeO_2-TiO_2 sample calcined at 773 K shows the typical spectra of TiO_2 anatase (space group $I4_1/amd$)[40] and CeO_2.[45] The Raman bands pertaining to the anatase phase appear at 147, 196, 397, 514, and 638 cm^{-1}, whereas ceria exhibits peaks at 272, 463, and 570 cm^{-1}, which are in agreement with the literature report.[45] To explain the presence of ceria Raman peaks, it is necessary to recall its space group and vibrational

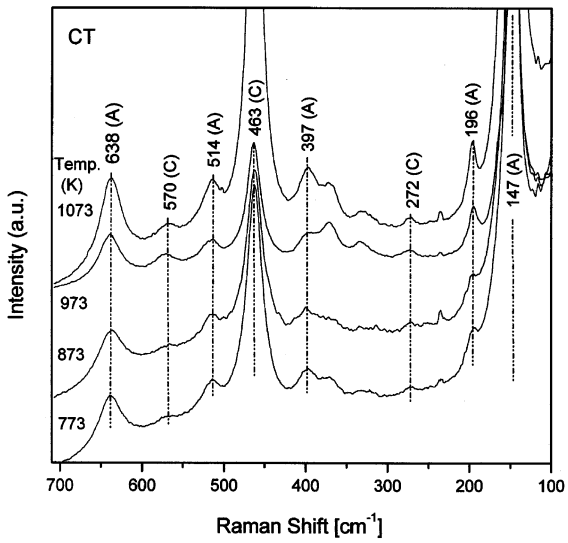

Figure 3. Raman spectra of CeO_2-TiO_2 (CT) calcined at different temperatures: (C) Lines due to CeO_2; (A) lines due to TiO_2 anatase.

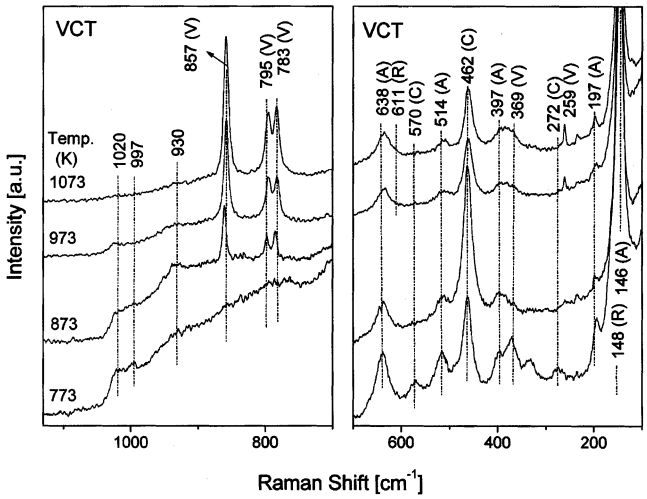

Figure 4. Raman spectra of 5% V_2O_5/CeO_2-TiO_2 (VCT) calcined at different temperatures: (C) Lines due to CeO_2; (A) lines due to TiO_2 anatase; (R) lines due to TiO_2 rutile; (V) lines due to $CeVO_4$.

modes. Ceria crystallizes in the cubic fluorite-type lattice and belongs to the space group $Fm3m$.[45] This structure possesses six optical-phonon branches, among which three zone-center frequencies at ca. 272, 463, and 595 cm^{-1} are ascribed to the doubly degenerate TO (transverse optical) mode, the triply degenerate Raman-active mode, and the nondegenerate LO (longitudinal optical) mode, respectively.[46] In general, the Raman mode at ca. 463 cm^{-1} can be directly detected by spectral measurements. This mode, assigned to F_{2g} symmetry, can be viewed as a symmetric breathing mode of the oxygen atoms around cerium ions. McBride et al.[47] reported the Raman spectra of $Ce_{1-x}RE_xO_{2-y}$ (RE = rare earth) solid solutions and found that the F_{2g} mode becomes asymmetric with the presence of a long low-frequency tail as x increases, and there is also a weak shoulder on the high-frequency side of the band, which would evolve into a broad peak at ca. 570 cm^{-1} for a larger x. This broad peak is associated with oxygen vacancies in the solid solutions.[46,48] A similar phenomenon is apparent in the present study. The XPS measurements presented in the latter paragraphs provide information about the formation of Ce^{3+} ions, supporting this observation. In line with XRD results, there are a few extra Raman bands that could not be assigned to any known compounds.

TABLE 2: XPS Core-Level Binding Energies (eV) of CeO_2-TiO_2 and V_2O_5/CeO_2-TiO_2 Samples Calcined at Different Temperatures

	binding energy (ev)			
temp (K)	O 1s	Ti $2p_{3/2}$	Ce 3d	V 2p
		CeO_2-TiO_2		
773	530.0	458.7	882.0	
873	530.1	458.7	881.6	
973	530.0	458.9	881.6	
1073	530.3	459.1	881.8	
		V_2O_5/CeO_2-TiO_2		
773	530.5	458.8	881.9	517.6
873	530.4	458.5	881.7	517.4
973	530.4	458.3	881.5	517.3
1073	530.8	458.3	882.2	517.2

As presented in Figure 4, the Raman spectra of the V_2O_5/CeO_2-TiO_2 sample calcined at 773 K exhibit prominent peaks due to the titania anatase phase and the ceria cubic phase along with broad and less intense bands in the region of ~930 and 995−1020 cm^{-1}. With increasing calcination temperature, the intensity of the bands pertaining to anatase and ceria increases proportionately, whereas the broad bands around 930 and 995−1020 cm^{-1} disappear progressively. At a calcination temperature of 873 K, a few new peaks could be seen at ~234, 260, 372, 783, 795, and 857 cm^{-1}. These are the characteristic bands of the $CeVO_4$ phase.[51] The intensity of these bands increases with increasing calcination temperature. According to literature reports, the TiO_2 rutile phase (space group $P4_2/mnm$) exhibits bands at 144, 148, and 611 cm^{-1}, whose presence could be seen at 1073 K with very weak bands, in agreement with XRD results.[40] No strongly crystalline V_2O_5 features (Raman bands at ~995, ~702, ~527, ~404, ~284, and ~146 cm^{-1}) are apparent, in line with the XRD observations.[49,50] Generally, the Raman bands of supported metal oxide catalysts in the range of 1050−950 cm^{-1} are assigned to the stretching mode of the short terminal M═O bonds, whereas the bands in the range of 950−750 cm^{-1} are attributed to either the antisymmetric stretch of M−O−M bonds or the symmetric stretch of $(-O-M-O-)_n$ bonds.[52,53] The presence of weak bands at ~930 and ~995−1020 cm^{-1} in the case of 773−973 K calcined samples can be assigned to the dispersed vanadia on the surface of the mixed-oxide support, whose presence could not be found at 1073 K. At higher calcination temperatures, the dispersed vanadia interacts with the ceria portion of the mixed oxide, leading to the formation of the $CeVO_4$ stable compound. At low calcination temperatures, the impregnated vanadia is mostly in a highly dispersed state (polyvanadate) on the surface of CeO_2-TiO_2. Similar findings were also reported by Banares and Wachs for dehydrated VO_x/CeO_2 catalysts.[49,54] By employing in situ Raman spectroscopy, they demonstrated the disappearance of surface vanadium oxide species with the simultaneous formation of a bulk $CeVO_4$ phase (Raman peaks at 840, 774, 768, 458, 369, 259, 215, and 146 cm^{-1}) with increasing calcination temperature.[54] Raman is particularly powerful in the identification of the structure of amorphous systems that cannot be discerned by diffraction studies. On the whole, Raman spectra corroborate well with the XRD results.

To understand the nature of interactions between the supported oxide and the supporting oxides, samples of CeO_2-TiO_2 and 5% V_2O_5/CeO_2-TiO_2 calcined at different temperatures have been investigated by XPS technique. The electron-binding energies (eV) of the photoelectron peaks pertaining to O 1s, Ti 2p, Ce 3d, and V 2p are shown in Table 2 and agree well with the values reported in the literature.[31,32,55] The representative photoelectron peaks of O 1s and Ce 3d pertaining to both the

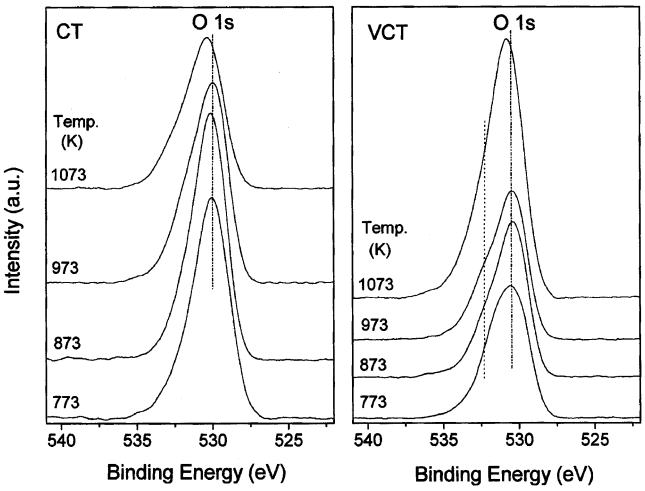

Figure 5. O 1s XPS spectra of CeO_2-TiO_2 (CT) and 5% V_2O_5/CeO_2-TiO_2 (VCT) samples calcined at different temperatures.

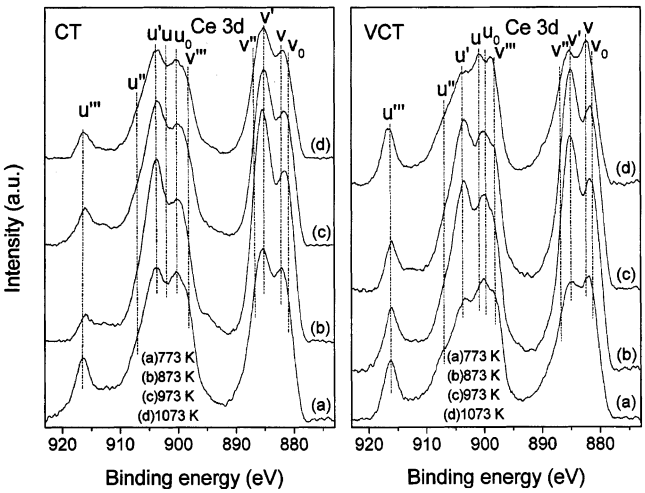

Figure 6. Ce 3d XPS spectra of CeO_2-TiO_2 (CT) and 5% V_2O_5/CeO_2-TiO_2 (VCT) samples calcined at different temperatures.

CeO_2-TiO_2 and 5% V_2O_5/CeO_2-TiO_2 samples are depicted together in Figures 5 and 6, respectively. Figure 5 displays the O 1s XP spectra of CeO_2-TiO_2 and 5% V_2O_5/CeO_2-TiO_2 samples calcined at different temperatures. As shown in Figure 5, the O 1s peak is, in general, broad and complicated because of the nonequivalence of surface oxygen ions. The peak shape suggests that it is composed of more than one peak arising from the overlapping contribution of oxygen from ceria, titania, and amorphous Ce−Ti−O compounds in the case of the CeO_2-TiO_2 support. The binding energy of the most intense O 1s peak slightly increased for the 1073 K calcined sample. Similarly, the O 1s profile of the V_2O_5/CeO_2-TiO_2 sample is further complicated because of the overlapping contribution of oxygen from various component oxides. The broad peak (indicated by a dotted line in the Figure) on the higher binding-energy end can be attributed to the formation of the $CeVO_4$ compound, usually observed around 532.9 eV.[41] The Ti 2p photoemission spectra of the support exhibited (not shown) typical XPS peaks in the range of 458.7−459.1 eV for Ti $2p_{3/2}$; these agree well with the values reported in the literature.[20,21] The intensity of the Ti 2p core-level spectra increased with increasing calcination temperature because of better crystallization of TiO_2. In the case of V_2O_5/CeO_2-TiO_2 samples, the binding energy of the Ti $2p_{3/2}$ peak varied between 458.8 and 458.3 eV. These values are within the range reported in the literature for stoichiometric TiO_2 surfaces.[20,21,31,32] Hence, it can be inferred from XPS results that titanium is mostly confined to its highest oxidation state (IV).

The Ce 3d XP spectra of CeO_2-TiO_2 and 5% V_2O_5/CeO_2-TiO_2 samples calcined at different temperatures are shown in Figure 6. The XPS core-level spectra of Ce 3d are generally characterized by complex but distinct features that are related to the final-state occupation of the Ce 4f level.[56] On the basis of the works of Burroughs et al.,[57] Pfau and Schierbaum,[55] and Creaser et al.,[58] the Ce 3d spectrum can be assigned as follows: The peaks labeled u are due to $3d_{3/2}$ spin−orbit states, and those labeled v are the corresponding $3d_{5/2}$ states. The u‴/v‴ doublet is due to the primary photoemission from Ce(IV)-O_2. The u/v and u″/v″ doublets are shakedown features resulting from the transfer of one or two electrons from a filled O 2p orbital to an empty Ce 4f orbital. The u′/v′ doublet is due to photoemission from Ce (III) cations. The Ce 3d spectrum of the CeO_2-TiO_2 sample basically denotes a mixture of Ce^{3+}/Ce^{4+} oxidation states giving rise to a myriad of peaks indicating that the surface of the sample is not fully oxidized. With increasing calcination temperature, the intensity of the u′/v′ doublet due to primary photoemission from Ce^{3+} relative to the intensities of the peaks due to photoemission from Ce^{4+} (u‴/v‴) increases gradually up to 873 K and then decreases. An additional less-resolved peak centered at 880.9 eV can be observed in the spectrum. This peak is a shakedown feature resulting from the transfer of one electron from a filled O 2p orbital to a Ce 4f orbital during photoemission from Ce^{3+} cations. This shakedown feature gives rise to an additional doublet, which is labeled as u_0/v_0 in the spectrum. The presence of u_0/v_0 and u′/v′ doublet peaks in the spectrum indicates that the CeO_2-TiO_2 sample contains some oxygen vacancies and is in a partially reduced state. Partial photoreduction of CeO_2 during XPS measurements is a well-known fact in the literature.[59−61] The reduction is mainly due to the progressive elimination of surface hydroxyls and oxygen ions from the CeO_2 surface upon vacuum treatment. The Ce 3d spectra of vanadia-impregnated samples are fairly similar to the spectra of the CeO_2-TiO_2 support. With increasing calcination temperature, an increase in the intensity of the Ce^{3+} designated peaks is observed up to 973 K. This can be attributed primarily to the formation of the $CeVO_4$ compound. The Ce 3d spectrum of the 1073 K calcined sample was poorly resolved, which could be due to the incorporation of titanium cations into the ceria lattice in addition to the formation of the $CeVO_4$ compound.

The core-level spectra of V 2p (not shown) were observed to be broad in the case of V_2O_5/CeO_2-TiO_2 samples, which could be due to the presence of multiple oxidation states or charge transfer between the active component and the support (metal oxide−support oxide interaction).[62−64] However, the intensity of the spectra increased with increasing calcination temperature. The V 2p BE values as presented in Table 2 indicate that vanadium is predominantly in the V(V) oxidation state. The BE of V $2p_{3/2}$ reported for the V(V) oxidation state ranges between 517.4−516.4 eV.[62−64] The BE values as presented in Table 2 and an increase in the intensity with increasing calcination temperature support the formation of $CeVO_4$, as observed from other techniques. Thus, the XPS results support the conclusions drawn from XRD and Raman results fairly well.

Conclusions

The CeO_2-TiO_2 mixed oxide is thermally stable, retaining its component oxides from poorly crystalline to well-crystallized

phases with increasing calcination temperature from 773 to 1073 K. The *a* cell-parameter values indicate some incorporation of titanium into the ceria lattice. However, no defined mixed phases could be observed from XRD and Raman studies. Impregnating vanadia on the CeO_2-TiO_2 mixed oxide enhances the crystallization of CeO_2 and TiO_2 oxides. No crystalline V_2O_5 could be observed from XRD and RS measurements irrespective of the calcination temperature. Furthermore, Raman results reveal that the dispersed vanadium oxide is mostly in the form of polyvanadate species on the surface of CeO_2-TiO_2 at lower calcination temperatures. The characterization results further suggest that the dispersed vanadium oxide interacts preferably with the ceria portion of the CeO_2-TiO_2 mixed oxide and forms a stable $CeVO_4$ compound at higher calcination temperatures. The XPS electron-binding energies indicate that CeO_2-TiO_2 and V_2O_5/CeO_2-TiO_2 samples calcined at 773 K mainly contain the mixed-oxide elements in their highest oxidation states, Ce(IV), Ti(IV), and V(V). The presence of Ce(III) has been noticed in both cases at all temperatures in different proportions. Additional studies are required to understand the mechanism of the solid-state reactions between the dispersed vanadium oxide and the CeO_2-TiO_2 mixed-oxide support because these materials are very promising for various catalytic purposes.[65]

Acknowledgment. B.M.R. acknowledges visiting fellowships from the Japan Science and Technology Corporation (JST), Japan, and the Centre National de la Recherche Scientifique (CNRS), France. A.K. thanks the Department of Science and Technology, New Delhi, for a Junior Research Fellowship in SERC scheme (SP/S1/H-20/98).

References and Notes

(1) Trovarelli, A. *Catal. Rev. Sci. Eng.* **1996**, *38*, 439 and references therein.

(2) Nunan, J. G.; Robota, H. J.; Cohn, M. J.; Bradley, S. A. *J. Catal.* **1992**, *133*, 309.

(3) Serre, C.; Garin, F.; Belot, G.; Marie, G. *J. Catal*. **1993**, *141*, 9.

(4) Monteiro, R. S.; Dieguez, L. C.; Schmal, M. *Catal. Today* **2001**, *65*, 77.

(5) Imamura, S.; Fakuda, I.; Ishida, S. *Ind. Eng. Chem. Res.* **1988**, *27*, 718.

(6) Mishra, V. S.; Mahajani, V. V.; Joshi, J. B. *Ind. Eng. Chem. Res.* **1995**, *34*, 2.

(7) Trovarelli, A.; Dolcetti, G.; de Leitenburg, C.; Kaspar, J.; Finetti, P.; Santoni, A. *J. Chem. Soc., Faraday Trans. 1* **1992**, *88*, 1311.

(8) Zwinkels, M. F. M.; Jaras, S. G.; Menon, P. G. *Catal. Rev. Sci. Eng*. **1993**, *35*, 319.

(9) Mackrodt, W. C.; Fowles, M.; Morris, M. A. European Patent 91,-307,165, 1991.

(10) Laachir, A.; Perrichon, V.; Badri, A.; Lamotte, J.; Catherine, E.; Lavalley, J. C.; El Fallah, J.; Hilarie, L.; Leonormand, F.; Quemere, E.; Sauvion, G. N.; Touret, O. *J. Chem. Soc., Faraday Trans. 1* **1991**, *87*, 1601.

(11) Kubsh, J. E.; Rieck, J. S.; Spencer, N. D. *Stud. Surf. Sci. Catal.* **1994**, *71*, 109.

(12) Sauvion, G. N.; Caillod, J.; Gourlaouen, C.; Rhone-Poulenc. European Patent 0207,857, 1986.

(13) Ohata, T.; Tsuchitani, K.; Kitayuchi, S.; Nippon, S. K. Japanese Patent 8,890,311, 1988.

(14) Ashley, N. E.; Rieck, J. S. Grace W. R. and Co-Conn. U.S. Patent 484,727, 1991.

(15) Cho, B. K. *J. Catal.* **1991**, *131*, 74.

(16) Connell, M. O.; Morris, M. A. *Catal .Today* **2000**, *59*, 387.

(17) Rynkowski, J.; Farbotko, J.; Touroude, R.; Hilaire, L. *Appl. Catal., A* **2000**, *203*, 335.

(18) Pijolat, M.; Prin, M.; Soustelle, M.; Tourer, O.; Nortier, P. *J. Chem. Soc. Faraday Trans.* **1995**, *91*, 3941.

(19) Wong, G. S.; Vohs, J. M. *Surf. Sci*. **2002**, *498*, 266.

(20) Biener, J.; Baumer, M.; Wang, J.; Madrix, R. J. *Surf. Sci*. **2000**, *450*, 12.

(21) Wang, Q.; Madrix, R. J. *Surf. Sci*. **2001**, *474*, L213.

(22) Védrine, J. C. *Catal. Today* **1994**, *20*, 1.

(23) Gellings, P. J. In *Catalysis*; Bond, G. C., Webb, G., Eds.; The Royal Society of Chemistry: London, 1985; Vol. 7, p 105.

(24) Bond, G. C.; Tahir, S. F. *Appl. Catal.* **1991**, *71*, 1 and references therein.

(25) Bosch, H.; Janssen, F. *Catal. Today* **1988**, *2*, 369.

(26) Eon, J. G.; Olier, R.; Volta, J. C. *J. Catal.* **1994**, *145*, 318.

(27) Kung, H. H.; Kung, M. C. *Appl. Catal., A* **1997**, *157*, 105.

(28) Khodakov, A.; Olthof, B.; Bell, A. T.; Iglesia, E. *J. Catal.* **1999**, *181*, 205.

(29) Zhao, Z.; Yamada, Y.; Teng, Y.; Ueda, A.; Nakagawa, K.; Kobayashi, T. *J. Catal.* **2000**, *190*, 215.

(30) Klug, H. P.; Alexander, L. E. *X-ray Diffraction Procedures for Polycrystalline and Amorphous Materials*, 2nd ed.; Wiley & Sons: New York, 1974.

(31) *Practical Surface Analysis*, 2nd ed.; Briggs, D., Seah, M. P., Eds.; Auger and X-Ray Photoelectron Spectroscopy; Wiley: New York, 1990; Vol. 1.

(32) Wagner, C. D.; Riggs, W. M.; Davis, L. E.; Moulder, J. F. In *Handbook of X-ray Photoelectron Spectroscopy*; Muilenberg, G. E., Ed.; Perkin-Elmer Corporation: Eden Prairie, Minnesota, 1978.

(33) Reddy, B. M.; Manohar, B.; Reddy, E. P. *Langmuir* **1993**, *9*, 1781.

(34) Reddy, B. M.; Ganesh, I.; Reddy, E. P. *J. Phys. Chem. B* **1997**, *101*, 1769.

(35) Preuss, A.; Gruehn, R. *J. Solid State Chem.* **1994**, *110*, 363.

(36) Hadjiivanov, K. I.; Klissurski, D. G. *Chem. Soc. Rev.* **1996**, *25*, 61 and references therein.

(37) Lin, J.; Yu, J. C. *J. Photochem. Photobiol., A* **1998**, *116*, 63.

(38) Anderson, C.; Bard, A. J. *J. Phys. Chem.* **1994**, *98*, 1769.

(39) De Faria, L. A.; Trasatti, S. *J. Colloid. Interface Sci.* **1994**, *167*, 352.

(40) Kosmulski, M. *Adv. Colloid Interface Sci.* **2002**, *99*, 255.

(41) Reddy, B. M.; Khan, A.; Yamada, Y.; Kobayashi, T.; Loridant, S.; Volta, J. C. *J. Phys. Chem. B* **2002**, *106*, 10964.

(42) Reddy, B. M.; Khan, A.; Yamada, Y.; Kobayashi, T.; Loridant, S.; Volta, J. C. *Langmuir* **2003**, *19*, 3025.

(43) Bozo, C.; Gaillard, F.; Guilhaume, N. *Appl. Catal., A* **2001**, *220*, 69.

(44) Colon, G.; Pijolat, M.; Valdivieso, F.; Vidal, H.; Kaspar, J.; Finocchio, E.; Daturi, M.; Binet, C.; Lavalley, J. C.; Baker, R. T.; Bernal, S. *J. Chem. Soc., Faraday Trans*. **1998**, *94*, 3717.

(45) Lin, X.-M.; Li, L.-P.; Li, G.-S.; Su, W.-H. *Mater. Chem. Phys*. **2001**, *69*, 236.

(46) Weber, W. H.; Hass, K. C.; McBride, J. R. *Phys. Rev. B* **1993**, *48*, 178.

(47) McBride, J. R.; Hass, K. C.; Poindexter, B. D.; Weber, W. H. *J. Appl. Phys.* **1994**, *76*, 2435.

(48) Spanier, J. E.; Robinson, R. D.; Zhang, F.; Chan, S.-W.; Herman, I. P. *Phys. Rev. B* **2001**, *64*, 245407.

(49) Banares, M. A.; Wachs, I. E. *J. Raman Spectrosc.* **2002**, *33*, 359.

(50) Olthof, B.; Khodakov, A.; Bell, A. T.; Iglesia, E. *J. Phys. Chem. B* **2000**, *104*, 1516.

(51) Hirata, T.; Watanabe, A. *J. Solid State Chem*. **2001**, *158*, 254.

(52) Knözinger, H.; Mestl, G. *Top. Catal*. **1999**, *8*, 45.

(53) Wachs, I. E. *Top. Catal*. **1999**, *8*, 57.

(54) Banares, M. A.; Martinez-Huerta, M. V.; Gao, X.; Fierro, J. L. G.; Wachs, I. E. *Catal. Today* **2000**, *61*, 295.

(55) Pfau, A.; Schierbaum, K. D. *Surf. Sci.* **1994**, *321*, 71.

(56) Mullins, D. R.; Overbury, S. H.; Huntley, D. R. *Surf. Sci.* **1998**, *409*, 307.

(57) Burroughs, A.; Hamnett, A.; Orchard, A. F.; Thornton, G. *J. Chem. Soc., Dalton Trans*. **1976**, *1*, 1686.

(58) Creaser, D. A.; Harrison, P. G.; Morris, M. A.; Wolfindale, B. A. *Catal. Lett.* **1994**, *23*, 13.

(59) Paparazzo, E.; Ingo, G. M.; Zacchetti, N. *J. Vac. Sci. Technol., A* **1991**, *9*, 1416.

(60) Park, P. W.; Ledford, J. S. *Langmuir* **1996**, *12*, 1794.

(61) Fierro, J. L. G.; Soria, J.; Sanz, J.; Rojo, J. M. *J. Solid State Chem*. **1987**, *66*, 154.

(62) Nag, N. K.; Massoth, F. E. *J. Catal*. **1990**, *124*, 127.

(63) Bukhtiyarov, V. I. *Catal. Today* **2000**, *56*, 403.

(64) Reddy, B. M.; Ganesh, I.; Reddy, E. P.; Fernández, A.; Smirniotis, P. G. *J. Phys. Chem. B* **2001**, *105*, 6227.

(65) Guglielminotti, E.; Boccuzzi, F. *J. Mol. Catal. A: Chem.* **1996**, *104*, 273.